

Quasiresonance: Switching Internal Energy Transfer On and Off[†]

Antonia Ruiz^{‡,§} and Eric J. Heller^{*,‡,#}

Department of Physics, Harvard University, Cambridge, Massachusetts 02138, Departamento de Física Fundamental y Experimental, Electrónica y Sistemas, Universidad de La Laguna, La Laguna 38203, Tenerife, Spain, and Department of Chemistry and Chemical Biology, Harvard University, Cambridge, Massachusetts 02138

Received: July 7, 2005; In Final Form: October 22, 2005

Quasiresonance involves a slow “external” switching on and off of an interaction between internal degrees of freedom described by action-angle variables having approximate resonances. The resonances or near-resonances spawn slow coordinates that fail to be adiabatic, but the remaining coordinates may be fast enough to have conserved actions. The interaction either can be imposed externally as a time dependent coupling or can arise autonomously due to interactions with other degrees of freedom. A resonance transformation into slow and fast angles reveals the action corresponding to the fast angle is adiabatic and conserved to very high accuracy. This paper extends our work on quasiresonance to new systems and regimes, including the He–H₂ system, collisions with a periodic lattice, perturbative interactions, and discussion of quasiresonance in higher dimensional systems.

1. Introduction

Quasiresonant vibration–rotation energy transfer (QRVT) was discovered experimentally^{1,2} in the context of low velocity inelastic collisions between an atom and a vibro-rotationally excited diatomic molecule. In these collisions, certain vibration–rotation transitions dominate all others, which would nominally be allowed, over a significant range of initial conditions. The first experimental evidence of QRVT¹ was reported in a level-resolved study of vibro-rotationally inelastic collisions between Li₂^{*} and noble gas atoms. A strong correlation between the change in the rotational (*j*) and vibrational (*v*) quantum numbers of the diatomic at the most important peak of the final rotational states was also observed, with the propensity rule $\Delta j = -\Delta v$. Experimental results obtained for different collision species show a remarkable insensitivity to both the initial vibrational state and the nature of the interaction potential.^{1,3,4} A QRVT type mechanism provides a path to selectively populate extremely high rotational states of molecules not easily reached by direct rotational excitation.⁵

The striking properties of quasiresonant vibro-rotational energy transfer have stimulated a number of theoretical studies,^{2,6–11} both classical trajectories analysis and quantum mechanical computations, of inelastic cross sections and rate coefficients for collisions between one atom and a rotationally excited diatom at ordinary and ultracold temperatures. The good qualitative agreement between classical and quantum results found so far suggests that the classical dynamics of the system is playing a significant role in the mechanism underlying the QRVT energy transfer.

In a recent paper¹² the present authors have extended the theory of quasiresonance to nonautonomous systems and have further explored the theory and numerics of the phenomenon. Here, after a brief review of quasiresonance, we consider two

additional systems: collision of an atom with a lattice and the perturbative regime, where we encounter some rather bizarre quasiresonant behavior of what we call “Diophantine” integrals.

2. Basics of Quasiresonance

The quasiresonance phenomenon may be understood as an extension of the classical adiabatic theorem to systems with at least one “slow” coordinate, i.e., one which is not adiabatic. Thus, the actions of the slow coordinate(s) will change as some interaction is turned on and off. Does that ruin any application of classical adiabaticity? Not if fast coordinates remain! They still can be treated adiabatically, and the method of averaging the potential over the fast motion suggests itself. This average often has a very pretty physical interpretation, as we will show.

Note that it is not always possible to turn on and off interactions so slowly that all coordinates become adiabatic, because when resonances are present there are coordinates with effectively zero frequency, slower than which nothing can be. The harbinger of this exists already in one dimension, in the case of a double well potential. Motion at the energy of the separatrix will not be adiabatic, due to the vanishing of the classical frequency.

Consider a time dependent potential, which turns on and then off, and which internally couples some system of two or more degrees of freedom. There are many possible outcomes, depending on the strength, form, and duration of the interaction, the classical frequencies of the system, its internal phase space structure, etc. Assuming there are initially good actions in the system,

(i) the interaction time may be fast compared to any coordinate and no action is generally conserved, or

(ii) the interaction time may be slow compared to any coordinate (i.e., there are no resonance conditions in the system, either initially or during the interaction) and all actions are generally conserved, or

(iii) the interaction time may be slow compared to some coordinates and fast compared to others, throughout the interaction. Some corresponding “fast” actions will be conserved.

[†] Part of the special issue “Jack Simons Festschrift”.

^{*} Corresponding author.

[‡] Department of Physics, Harvard University.

[§] Universidad de La Laguna.

[#] Department of Chemistry and Chemical Biology, Harvard University.

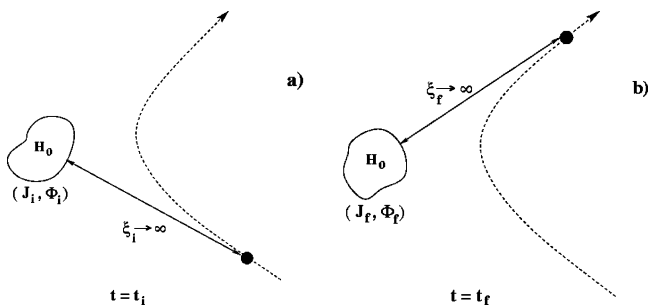


Figure 1. Sketch of the initial (a) and final (b) states in the transient interaction process between the system H_0 and a structureless incoming particle.

In the last case, it can happen that

(i) the slow coordinates are intrinsically slow (i.e., they did not become slow out of resonance between two “fast” coordinates), or

(ii) some of the slow coordinates did arise out of resonance or near resonance (quasiresonance) between two or more “fast” coordinates.

It is this last, ubiquitous situation that is our concern. A slow coordinate arises in the following example, which will serve to illustrate the general phenomena. Consider a two-dimensional integrable system H_0 , perturbed by the transient interaction with one structureless particle. The Hamiltonian of the total system may be expressed as

$$H = H_0(\mathbf{J}) + H_k(\mathbf{P}) + \epsilon V(\mathbf{J}, \Phi, \mathbf{P}, \mathbf{Q}; \xi) \quad (1)$$

where $\mathbf{J} \equiv (J_1, J_2)$ and $\Phi \equiv (\Phi_1, \Phi_2)$ are the action-angle variables that describe the unperturbed system H_0 , \mathbf{Q} and \mathbf{P} are the coordinate and the conjugate momentum (not necessarily action-angle variables) of the incoming particle, and H_k is its kinetic energy. ϵ is a small parameter that characterizes the magnitude of the interaction term. We will assume that the term satisfies the condition

$$\lim_{\xi \rightarrow \infty} V(\mathbf{J}, \Phi, \mathbf{P}, \mathbf{Q}; \xi) = 0 \quad (2)$$

with $\xi \equiv \xi(\mathbf{J}, \Phi, \mathbf{P}, \mathbf{Q})$ an *interaction parameter* that controls the amplitude of the interaction between the system H_0 and the particle. In a typical collisional process this parameter would correspond to the distance between centers of mass of the colliding species. Consider a collision in which the transient interaction of the system H_0 with the particle induces a change in its internal state from the initial state $(\mathbf{J}_i, \Phi_i) \equiv (J_{1i}, J_{2i}, \Phi_{1i}, \Phi_{2i})$ at $t = t_i$ ($\xi_i \rightarrow \infty$) to the final state $(\mathbf{J}_f, \Phi_f) \equiv (J_{1f}, J_{2f}, \Phi_{1f}, \Phi_{2f})$ at $t = t_f$ ($\xi_f \rightarrow \infty$), see Figure 1. We assume that the two independent frequencies of the unperturbed Hamiltonian H_0 satisfy an approximate resonance condition of the form

$$M\omega_2 - N\omega_1 \approx 0 \quad (3)$$

where

$$\omega_i(\mathbf{J}) = \frac{\partial H_0}{\partial J_i} \quad (i = 1, 2) \quad (4)$$

The secularity in the unperturbed Hamiltonian due to this resonance condition can be removed by applying standard secular perturbation theory.¹³ Namely, we can perform a canonical transformation from the variables (\mathbf{J}, Φ) to a new set of action-angle variables (\mathbf{I}, Φ) , which define a frame that rotates with the resonant frequency. Taking the generating function for

the canonical transformation as

$$F(\mathbf{I}, \mathbf{P}, \Phi, \mathbf{Q}) = (M\Phi_2 - N\Phi_1)I_1 + \Phi_2 I_2 + \mathbf{P} \cdot \mathbf{Q} \quad (5)$$

the equations for the transformation between the two sets of variables of the Hamiltonian H_0 are given by

$$\phi_1 = \frac{\partial F}{\partial I_1} = M\Phi_2 - N\Phi_1 \quad (6)$$

$$\phi_2 = \frac{\partial F}{\partial I_2} = \Phi_2 \quad (7)$$

$$J_1 = \frac{\partial F}{\partial \Phi_1} = -NI_1 \quad (8)$$

$$J_2 = \frac{\partial F}{\partial \Phi_2} = MI_1 + I_2 \quad (9)$$

In terms of the new variables the transformed Hamiltonian may be expressed as

$$H' = H_0(\mathbf{I}) + H_k(\mathbf{P}) + \epsilon V(\mathbf{I}, \Phi, \mathbf{P}, \mathbf{Q}; \xi) \quad (10)$$

If the approximate resonance condition (3) is satisfied, the evolution of the new angle variables in the rotating frame is given by

$$\dot{\phi}_1 = M\dot{\Phi}_2 - N\dot{\Phi}_1 \approx \epsilon \left(M \frac{\partial V}{\partial J_2} - N \frac{\partial V}{\partial J_1} \right) \quad (11)$$

and

$$\dot{\phi}_2 = \dot{\Phi}_2 = \omega_2(\mathbf{I}) + \epsilon \frac{\partial V}{\partial J_2} \quad (12)$$

Hence, provided that the frequency ω_2 is far enough from zero, the oscillation of the new angle variable ϕ_2 near the resonance will be fast compared to the variation of the angle variable ϕ_1 . Under these conditions, the dynamics of the system in the proximity of the nonlinear resonance can be described by the averaged Hamiltonian

$$\bar{H} = H_0(\mathbf{I}) + H_k(\mathbf{P}) + \epsilon \bar{V}(\mathbf{I}, \phi_1, \mathbf{P}, \mathbf{Q}; \xi) \quad (13)$$

where

$$\bar{V}(\mathbf{I}, \phi_1, \mathbf{P}, \mathbf{Q}; \xi) = \frac{1}{2\pi} \int_0^{2\pi} V(\mathbf{I}, \Phi, \mathbf{P}, \mathbf{Q}; \xi) d\phi_2 \quad (14)$$

Because \bar{H} does not depend on the angle variable ϕ_2 , its conjugated action variable I_2 is an adiabatic invariant of the motion in the proximity of the resonance. But, according to (8) and (9), this adiabatic invariance of the action conjugated to the fast angle variable ϕ_2 implies that

$$I_2 = J_2 + \frac{M}{N} J_1 = \text{const} \quad (15)$$

or

$$N\Delta J_2 + M\Delta J_1 = N(J_{2f} - J_{2i}) + M(J_{1f} - J_{1i}) = 0 \quad (16)$$

which gives the rational ratio in the action changes that is observed in the quasiresonance effect. Thus, a quasiresonance is implied by the existence of an adiabatic invariant character-

izing the quasiperiodic motion of the system, in the proximity of a nonlinear resonance between its internal degrees of freedom.

It is interesting that energy conservation (or here energy exchange between the system and the atom) is sacrificed in favor of conservation of the action I_2 of the system, because if $\Delta I_2 = (M/N)\Delta J_1 + \Delta J_2 = 0$, and therefore

$$\frac{\Delta J_2}{\Delta J_1} = -\frac{M}{N} \quad (17)$$

we have

$$\Delta E_{\text{sys}} = \omega_1 \Delta J_1 + \omega_2 \Delta J_2 = \Delta J_1 \left(\omega_1 - \frac{M}{N} N \omega_2 \right) \equiv -\Delta J_1 \omega_{\text{def}} = \Delta J_1 \frac{\dot{\phi}_1}{N} \quad (18)$$

where ω_{def} is the “defect” from perfect resonance.

Quasiresonance bears some relation with *adiabatic switching*,¹⁴ which is a method for semiclassical quantization that had some success in starting with a multidimensional separable problem of known quantized actions and switching on interactions adiabatically, hoping that the actions do not change, and thus allowing the energy with those actions to be read off of the trajectories that have suffered the switching. In that case the interaction is turned on and left on, and success is measured by the degree to which all the initial actions remain intact with the same values. Here, we have different goals, with physical systems in mind where the additional coupling turns on *and off* naturally. In quasiresonance, the system energy may not be conserved (although in an autonomous system the total energy of course is), and the actions change as well, with the caveat that ratios of action changes are special. In a sense we are tolerant of some action changes as long as other actions respond adiabatically, which means they stay constant and in so doing they impose the quasiresonant condition.

Here we present new results on the quasiresonance effect between the vibrational and rotational internal degrees of freedom of a diatom molecule in slow inelastic collisions with an external atom. We also consider the deflection on a plane of one atom due to the transient interaction potential generated by an infinite optical lattice, a nonautonomous system. Section 7 analyzes whether infinitely weak interactions are still quasiresonant. Finally, in section 8 we summarize the main conclusions of the work.

3. Examples of Quasiresonance

Once the specific mechanism for how the nonlinear resonance zones give quasiresonance has been elucidated and illustrated, in the following sections we present two examples of quasiresonance in autonomous and nonautonomous systems. As an example of a process that manifests the quasiresonance effect in a global autonomous system, we present the classical analysis of an atom–diatom inelastic collision, which reproduces some previous results by Forrey et al.⁷ In the case of quasiresonance arising from a nonautonomous transient interaction we will analyze the deflection on a plane of one atom by the weak interaction potential created by an infinite periodic lattice.

As an introduction to quasiresonance we consider the dynamics of an atom, fixed on a spring as it rotates on a plane, slightly perturbed by the collision with a slow incoming atom. Before the interaction occurs the dynamics of the unperturbed rotating atom is described by the integrable Hamiltonian

$$H_0 = H_0(J_r, J_\theta) = \frac{p_r^2}{2m} + \frac{p_\theta^2}{2mr^2} + U(r) \quad (19)$$

where m is the atom mass, p_r and p_θ are the momenta conjugated to the radial and angular variables r and θ , $U(r)$ is the internal elastic interaction potential, and

$$J_r = \frac{1}{2\pi} \oint p_r dr = \frac{1}{2\pi} \oint \sqrt{2m[H_0 - U(r)] - \frac{p_\theta^2}{r^2}} dr \quad (20)$$

and

$$J_\theta = \frac{1}{2\pi} \oint p_\theta d\theta = p_\theta \quad (21)$$

the vibrational and rotational action variables.

Initially, the atom is vibrating in and out as it rotates on a plane, tracing out a “gear” shape that is actually fixed in space if the radial and angular frequencies satisfy a resonance condition (3), see Figure 2a. More generally, the “gear” is slowly rotating clockwise or counterclockwise initially, with angular frequency $\dot{\phi}_1$, i.e., the slow angle. The gear-shaped potential is just the potential of the averaged Hamiltonian given in eq 13.

The interaction with the incoming particle induces a coupling between the internal degrees of freedom of the spinning atom and, therefore, a change in its vibrational and rotational frequencies. In the proximity of a resonance, when the condition $M\omega_r - N\omega_\theta \approx 0$ is satisfied, such variation produces a slow rotation of the *gear*, which starts moving as an effective *rigid rotor*, see Figure 2b. The angular momentum associated with this rotating gear is given by the new action variable I_θ , whereas the action conjugated to the rapid angle variable in the rotating coordinate system, in this system the radial or vibrational action, is the modified adiabatic invariant that satisfies the condition (15). Namely,

$$I_r = J_r + \frac{M}{N} J_\theta = \frac{1}{2\pi} \oint \sqrt{2m[H_0 - U(r)] - \frac{p_\theta^2}{r^2}} dr + \frac{M}{N} p_\theta = \text{const} \quad (22)$$

This example illustrates the physical nature of the reduced dimensionality system that results when the average over the fast variable is performed. As long as the quasiresonance holds, the reduced dimensionality object acts consistently as if it did not possess the degrees of freedom removed by averaging.

4. Quasiresonant Effect from He–H₂ Collision

In this section we present the classical analysis of the quasiresonant effect that arises in the vibrationally and rotationally inelastic collisions between the He atom and the diatom H₂. In the center of mass frame the Hamiltonian of the system can be written as

$$H = \frac{p_r^2}{2m} + \frac{j^2}{2mr^2} + \frac{P_R^2}{2\mu} + \frac{L^2}{2\mu R^2} + U(r) + V(r, R, \theta, \psi) \quad (23)$$

where r is the interatomic distance in the H₂ molecule, p_r is its conjugate momentum, θ is the angular coordinate of the molecular axis, R is the distance between the He atom and the center of mass of the diatom, P_R is its conjugate momentum, ψ is the external atom angular coordinate, m is the reduced diatom molecular mass, μ is the reduced mass of the He atom with

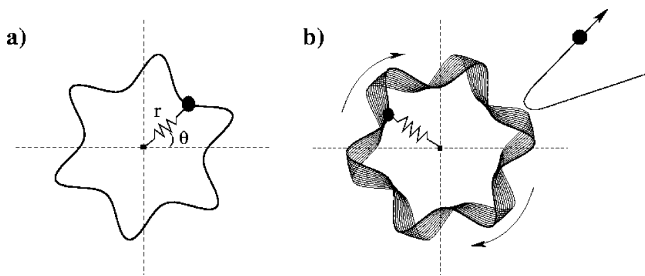


Figure 2. (a) Trajectory (a fixed “gear” shape) described by an atom fixed on a spring when there is an integer ratio of six between the vibrational and rotational frequencies. This is the form of the fast angle-averaged potential in the adiabatic analysis. (b) Sketch of the evolution of the vib-rotor after it is perturbed by a slow colliding particle.

respect to the diatom, $\mathbf{j} = j\hat{\mathbf{j}}$ is the diatom angular momentum, and $\mathbf{L} = L\hat{\mathbf{L}}$ is the orbital angular momentum of the He atom with respect to the diatom. As in ref 7, we have used in our simulations the interatomic potential $U(r)$ of Schwenke¹⁶ and the atom–diatom interaction potential $V(r, R, \theta, \psi)$ of Muchnick and Russek.¹⁷ For the sake of simplicity, and without loss of generality, we have confined the scattering process to a plane by setting the molecular and orbital angular momenta along the same direction.

We will assume that the initial and final positions of the colliding atom are sufficiently far from the diatom ($V \approx 0$ at $t \rightarrow \pm\infty$). Hence, in this example the quasiresonance effect arises between the *quasiresonant* vibrational and rotational degrees of freedom of the molecular system

$$H_0(\mathbf{J}) \equiv H_0(J_r, J_\theta) = \frac{p_r^2}{2m} + \frac{j^2}{2mr^2} + U(r) \quad (24)$$

which has well-defined radial (vibrational) and angular (rotational) action variables,

$$J_r = \frac{1}{2\pi} \oint p_r dr \quad (25)$$

and

$$J_\theta = \frac{1}{2\pi} \oint j d\theta \quad (26)$$

when it is perturbed by the transient (autonomous) interaction with the incoming atom

$$V(\mathbf{J}, \Phi, \mathbf{Q}; \xi) \equiv V(J_r, J_\theta, \Phi_r, \Phi_\theta, R, \psi; \xi) \quad (27)$$

where $\Phi \equiv (\Phi_r, \Phi_\theta)$ are the molecular angle variables.

Figure 3a displays the root-mean-square (rms) of the change in the diatomic angular and radial classical actions in a collision between H_2 and He at relative energy $E = 10^{-6} \text{ cm}^{-1}$, initial radial action J_r fixed to reproduce the vibrational molecular quantum number $v_i = 2$ by imposing the semiclassical quantization rule

$$J_r = \hbar \left(v_i + \frac{1}{2} \right) \quad (28)$$

and a continuous distribution of initial angular molecular action J_θ . The initial molecular quantum states correspond to the values of the angular actions that satisfy the quantization rule

$$J_\theta = \hbar j_i \quad (29)$$

with j_i the rotational molecular quantum number.

The different peaks in Figure 3 represent the change in radial and angular molecular actions due to the transient interaction with the colliding atom when a quasiresonant condition of the form

$$M\omega_\theta - N\omega_r \approx 0 \quad (30)$$

is satisfied. As expected, the main peaks in Figure 3 define a series of plateau regions (see Figure 4) where the ratio of the changes in the actions of the quasiresonant vibrational and rotational molecular degrees of freedom takes a different low order rational value given by the propensity rule

$$\frac{\Delta J_\theta}{\Delta J_r} = -\frac{M}{N} = -r \quad (31)$$

The location of the center of the main quasiresonance domains can be predicted in this system from the distribution of the vib-rotational molecular energy levels by imposing the condition

$$E(v_i + |\Delta v|, j_i - |\Delta j|) \approx E(v_i - |\Delta v|, j_i + |\Delta j|) \quad (32)$$

or, classically, if we take the action’s changes to be arbitrarily small, eq 18, the on-resonance condition

$$\Delta E_{\text{sys}} = 0 \quad (33)$$

Note that this condition is insensitive to the nature of the interaction potential and depends instead on the intrinsic frequencies of the system.

As Figure 3 shows, the action changes are quite small for the He– H_2 system in this range of angular momenta and at this collision energy, except near resonances. The collision is so slow compared to both the vibration and rotation of the molecule that one might be tempted to claim the collision is always adiabatic in both actions. This claim would be very nearly true over much of the space of initial conditions. However, the spawning of a slow coordinate when the two frequencies approximately satisfy a low order rational ratio, as labeled by the peaks in Figure 3, causes adiabaticity to break down. Figure 3a shows a schematic of the shape of the average potential at each of the resonance peaks for this case of a homonuclear diatomic molecule. It is clear that as the number of “teeth” in the gear increases, and the depth or radial variation of the teeth decreases, the nonadiabtic changes decrease at resonance. The shapes were generated using the same amplitude of vibrational motion in each case. For a given number of teeth, relatively shallow teeth form at higher rotational speeds because they are more rounded off by the motion.

Outside the quasiresonant zones the changes in j and v decrease several orders of magnitude and the correlation (31) that characterizes the quasiresonance effect practically disappears. This is shown in Figure 5 where a nearly perfect correlation between the changes in the molecular classical actions can be observed for the initial actions $J_{\theta_i} = 9$ ($r = 4.0008$) and $J_{\theta_i} = 22$ ($r = 2.0000$), but not for $J_{\theta_i} = 7$ and $J_{\theta_i} = 15$.

5. Grazing Collision: Deflection by a Transient Lattice

We next examine the weak interaction of an atom in two dimensions with a transient periodic lattice. An analogous autonomous system in one more degree of freedom is a grazing collision of an atom with a crystal surface.

Suppose we have one atom of mass m and energy E moving freely in a plane along the direction $\hat{\mathbf{p}}_i = (\hat{p}_x, \hat{p}_y) = (\cos \theta_i, \sin$

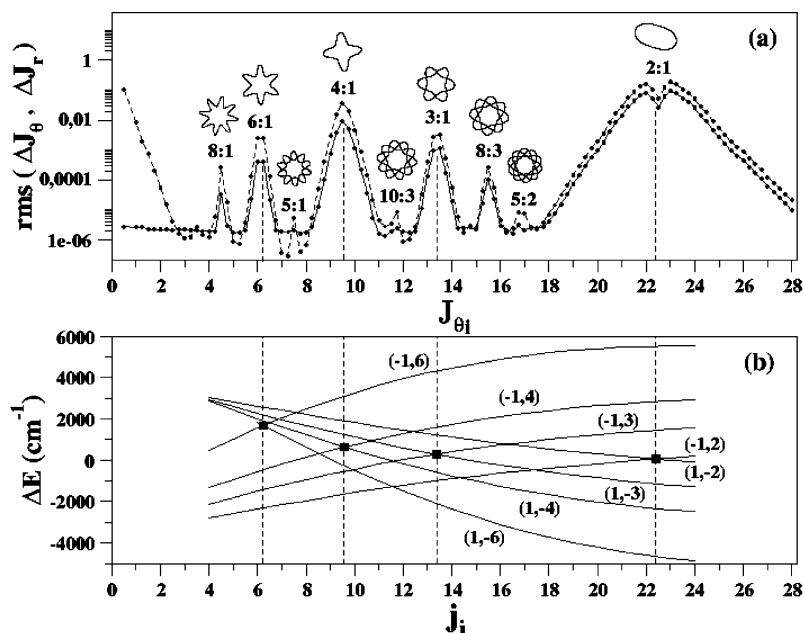


Figure 3. (a) Root-mean-square (rms) of the change in the angular and radial molecular actions, $\Delta J_\theta = J_{\theta_f} - J_{\theta_i}$ and $\Delta J_r = J_{r_f} - J_{r_i}$, in a collision process between H_2 and He at energy $E = 10^{-6} \text{ cm}^{-1}$ and initial molecular vibrational quantum number $v_i = 2$. For each value of the molecular actions the rms was computed using the data of 1000 classical trajectories with all the remaining initial conditions fixed at random. The solid line corresponds to the change in the angular action J_θ and the dashed line to the change in radial action J_r . The values of the integer numbers M and N ($M:N$) that characterize the propensity rule (31) around each peak are indicated. (b) Diatom vibro-rotational energy changes, $\Delta E = E(v_i + |\Delta v|, j_i + |\Delta j|) - E(v_i, j_i)$, for initial molecular vibrational quantum number $v_i = 2$ and different initial rotational quantum number j_i . The pairs of indexes indicate $(\Delta v, \Delta j)$ and the full squares show the positions where the relation (32) is satisfied. A schematic of the shape of the potential averaged over the fast angle at each of the resonance peaks is also given.

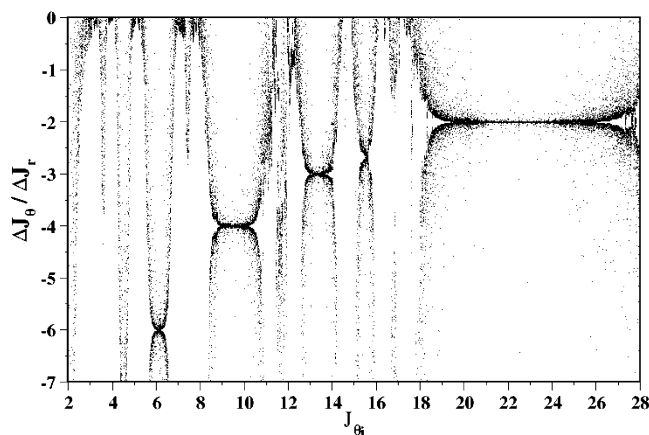


Figure 4. Ratio of molecular action changes $\Delta J_\theta / \Delta J_r$ vs the initial angular action J_{θ_i} for five of the classical trajectories included in Figure 3.

θ_i). We slowly switch on and off an infinite periodic lattice. We assume that the lattice is weak compared to the energy, $v_0 \ll E$ and that the deflection of the atom is not large. After the lattice is switched off the atom continues in free motion, but now along the direction $\hat{p}_f = (\hat{p}_x, \hat{p}_y) = (\cos \theta_f, \sin \theta_f)$. The Hamiltonian that describes the system can be expressed as

$$H = H_0(p_x, p_y) + V(x, y, t) = \frac{1}{2m}(p_x^2 + p_y^2) + v_0 g(t) u(x, y) \quad (34)$$

where the interaction potential

$$u(x, y) = \cos^\eta x \cos^\eta y \quad (35)$$

The quasiresonant effect arises when the integrable system $H_0(J_1, J_2) \equiv H_0(p_x, p_y) = (1/2m)(p_x^2 + p_y^2)$ is perturbed by the transient (nonautonomous) interaction $V(\Phi; \xi) \equiv V(x, y; t) =$

$v_0 g(t) u(x, y)$ with $g(t)$ given by

$$g(t) = \exp[-(t - t_p)^2 / 2\sigma^2] \quad (36)$$

characterized by a parameter σ . For some incident angles the two unperturbed frequencies

$$\omega_i = \frac{\partial H_0}{\partial J_i} \equiv \frac{\partial H_0}{\partial p_i} = \frac{p_i}{m} \quad (i = x, y) \quad (37)$$

will satisfy a quasiresonant condition of the form $M\omega_x - N\omega_y \approx 0$.

Figures 6 and 7 display the variation of the root-mean-square of the change in the x -component of the momentum, $\Delta p_x = p_{x_f} - p_x$ (because the two components of the momentum are equivalent, we have only represented one of them), with respect to the incident direction and after the deflection process by two different sinusoidal lattices. Both pictures show significant changes in the component of the linear momentum of the atom for certain incident angles. In the first process ($\eta = 2$), we observe a series of relatively sparse peaks with very small variation of the component of the momentum in the regions between them. In the second case ($\eta = 8$), which gives a potential with much sharper peaks, there is a strong variation with the incident angle including some structure at the top of the highest peaks and larger action changes in the regions between them. The locations of the center of the most important peaks (dashed lines) are the same in the two cases and are given by the incident angles of the atom whose tangent,

$$\tan \theta_i = \frac{\omega_{y_i}}{\omega_{x_i}} = \frac{p_{y_i}}{p_{x_i}} = r \approx M/N \quad (38)$$

with M and N small integer values, implying a resonance condition between the two unperturbed frequencies of the

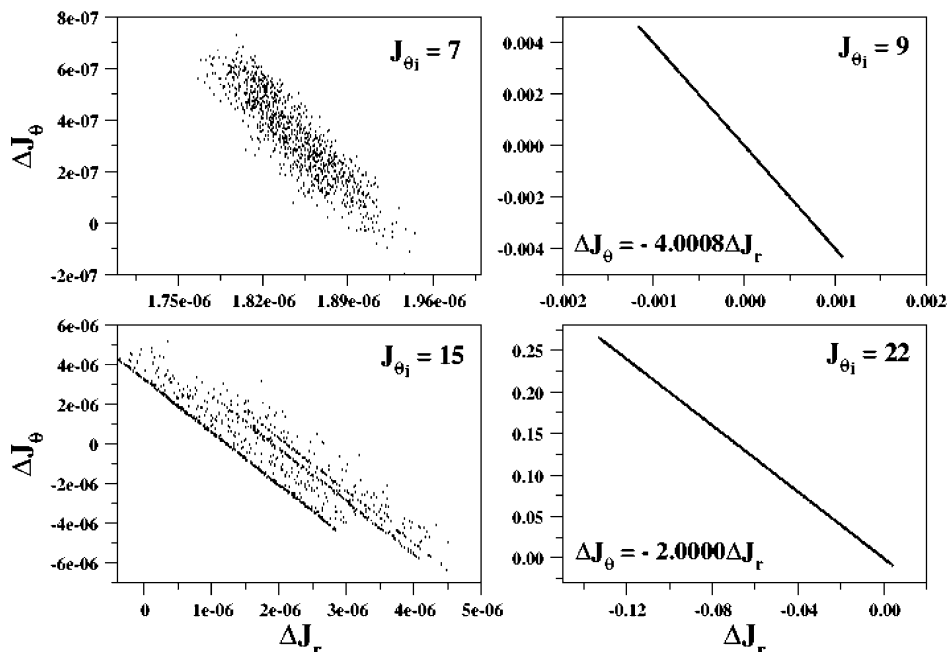


Figure 5. $\Delta J_\theta = J_{\theta_f} - J_{\theta_i}$ vs $\Delta J_r = J_{r_f} - J_{r_i}$ for different initial angular molecular actions in a scattering process between H_2 and He at energy $E = 10^{-6} \text{ cm}^{-1}$ and initial vibrational molecular state $v_i = 2$. The result of the linear fitting $\Delta J_\theta = -r\Delta J_r$ is indicated for the initial angular molecular actions $J_{\theta_i} = 9$ and $J_{\theta_i} = 22$.

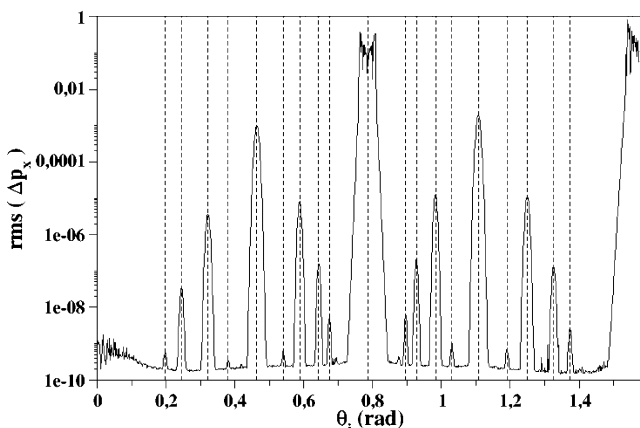


Figure 6. Root-mean-square (*rms*) of the change in the x-component of the momentum, $\Delta p_x = p_{x_f} - p_{x_i}$, vs the incident angle, for one atom of mass $m = 4.0026$ and energy $E = 20$, a coupling strength $v_0 = 0.1$, a Gaussian parameter $\sigma = 20$, and the interaction potential (35) with $\eta = 2$. The rms was obtained from 1000 trajectories with the same incident angle and initial positions chosen at random. The dotted lines give the position of the incident angles whose tangent is a rational number (38), $r = M/N$, with M and N small integers. All quantities are expressed in arbitrary units.

system. The potential obtained by averaging over the fast angle ϕ_2 is a periodic series of parallel ridges perpendicular to the slow angle, i.e., a one-dimensional pendulum Hamiltonian in the slow angle.

As Figures 8 and 9 show, the locations of the center of the main peaks in the variation of the components of the momentum of the atom correspond also to the centers of a series of plateau regions where the propensity rule

$$\frac{\Delta p_x}{\Delta p_y} = -\frac{M}{N} \quad (39)$$

is satisfied, with r the same rational value that appears in (38). The more sparse and smooth the peaks in the variation of the actions appear, i.e., the more isolated the main nonlinear

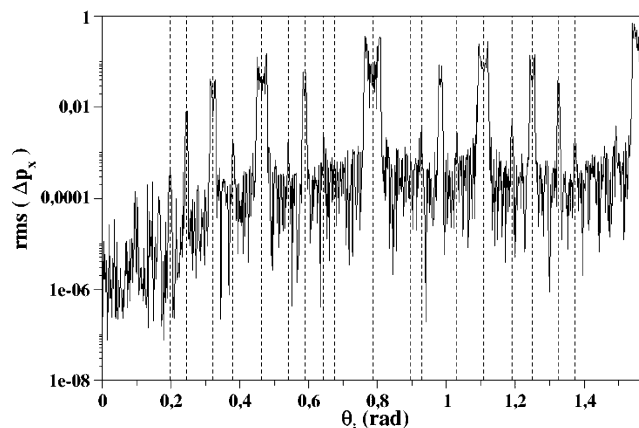


Figure 7. Same as Figure 6 but for a eighth power sinusoidal lattice ($\eta = 8$) in the interaction potential (35).

resonance zones are in phase space, the better defined are the corresponding plateau regions in ratio of action changes.

In this context we mention the work of Miklavc¹⁸ and McCaffery,^{8,19} who discuss the interesting perspective of atom–diatom quasisresonant vibration–rotation energy transfer as collisional state change consisting of momentum interconversion (linear-to-linear and angular) within constraints set by energy conservation. Translating these “momenta” as “actions”, their conclusions indeed fit within the present framework.

6. Grazing Collision: Weak Interaction Limit

The discussion so far should have left the definite impression that rational fractions and number theory are tied up in quasisresonance, as in other resonance phenomena. This is made very clear by the following perturbative analysis of quasisresonance in a collision with a transient lattice. In the process we also gain insight into the roles of the number of Fourier components in the perturbation potential (which controls the sharpness of the peaks) and the speed of the particle, i.e., the number of unit cells traversed while the interaction is on.

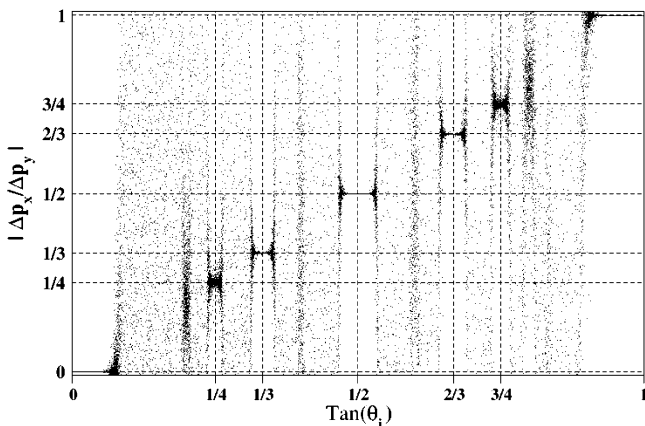


Figure 8. Dots give $\Delta p_x/\Delta p_y$ vs p_y/p_x . For each incident angle the data of 20 trajectories with initial position chosen at random are included. All the parameters are the same as in Figure 6. The straight solid line represents the curve $p_y/p_x = \Delta p_x/\Delta p_y$.

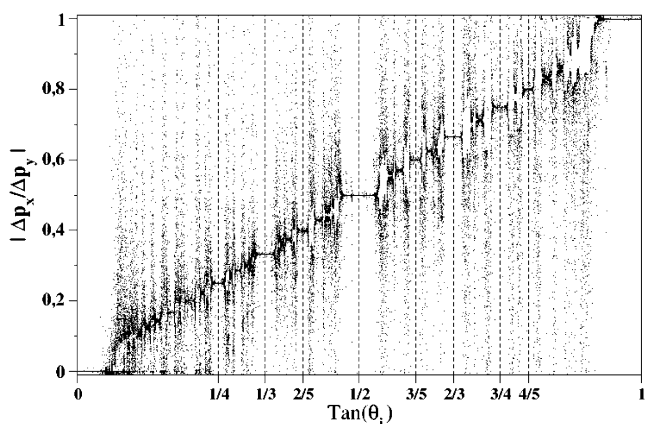


Figure 9. Same as Figure 8 but for an eighth power sinusoidal lattice ($\eta = 8$) in the interaction potential (35).

According to our previous results, nothing prevents the quiresonance effect from applying in the limit of a weak transient interaction. As befits first-order classical perturbation theory, we assume an unperturbed trajectory and compute the impulse due to the potential, applying *primitive* first-order classical perturbation theory to obtain the change in the actions $\mathbf{J} \equiv (J_1, J_2)$, $\mathbf{J} = \mathbf{J}_0 = \text{const}$, by means of the perturbation integral

$$\Delta J_i = -\frac{\partial}{\partial \Phi_{i_0}} \int_{-\infty}^{\infty} V(\mathbf{J}_0, \Phi_0 + \omega t; \xi(t)) dt \quad (i = 1, 2) \quad (40)$$

where $\Phi_0 \equiv (\Phi_{10}, \Phi_{20})$ are the initial angle variables and $\omega \equiv (\omega_1, \omega_2)$ are the frequencies associated with the unperturbed Hamiltonian $H_0 \equiv H_0(J_1, J_2)$. For the trajectory $\mathbf{r}(t) = \mathbf{r} + \mathbf{v}t$ ($\mathbf{v} = \text{const}$) passing through (x, y) at $t = 0$, with $\mathbf{v} = (\alpha, \beta)$ eq 40 takes the form for the potential $V(x, y) = \cos^\eta x \cos^\eta y$

$$\Delta J_1 = \Delta p_x = \frac{\partial}{\partial x} I_n(x, y; \alpha, \beta) \quad \Delta J_2 = \Delta p_y = \frac{\partial}{\partial y} I_n(x, y; \alpha, \beta) \quad (41)$$

where

$$I_n(x, y; \alpha, \beta) = \int_{-\infty}^{\infty} V(\mathbf{J}_0, \Phi_0 + \omega t; \xi(t)) dt = \int_{-\infty}^{\infty} e^{-r^2} \cos^\eta(x + \alpha t) \cos^\eta(y + \beta t) dt \quad (42)$$

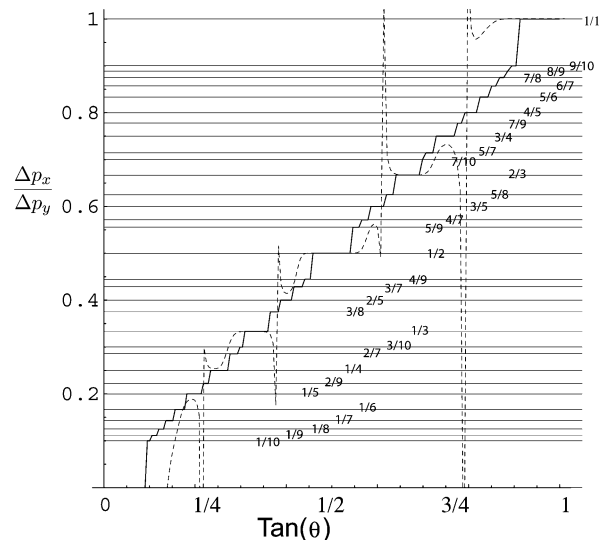


Figure 10. Devil's staircase of rational plateaus in $\Delta p_x/\Delta p_y$ for a tenth power sinusoidal lattice ($\eta = 10$); with $x = 0.12$, $y = 0.77$, and $|\mathbf{v}| = 130$; see eq 45 (solid line), and $|\mathbf{v}| = 10$ (dashed line).

Expanding the cosines as sums of complex exponentials, we find

$$I_n(x, y; \alpha, \beta) = 2^{-2n} \sum_{m, m'} \binom{n}{m} \binom{n}{m'} e^{i(n-2m)x + i(n-2m')y} e^{-(\alpha(n-2m) + \beta(n-2m'))^2/4} \quad (43)$$

The real exponents are the inner product (projection) of two vectors, $\mathbf{v} = (\alpha, \beta)$ and $\mathbf{k} = (n - 2m, n - 2m')$. In the new notation,

$$I_n(\mathbf{r}; \mathbf{v}) = 2^{-2n} \sum_{\mathbf{k}} C_n(\mathbf{k}) e^{i\mathbf{k}\mathbf{r}} e^{-(\mathbf{v}\cdot\mathbf{k})^2/4} \quad (44)$$

where $C_n(\mathbf{k}) = \binom{n}{m} \binom{n}{m'}$, and then

$$\frac{\Delta p_x}{\Delta p_y} = \frac{\sum_{\mathbf{k}} C_n(\mathbf{k}) k_x e^{i\mathbf{k}\mathbf{r}} e^{-(\mathbf{v}\cdot\mathbf{k})^2/4}}{\sum_{\mathbf{k}} C_n(\mathbf{k}) k_y e^{i\mathbf{k}\mathbf{r}} e^{-(\mathbf{v}\cdot\mathbf{k})^2/4}} = \frac{\sum_{\mathbf{k}} C_n(\mathbf{k}) (n - 2m) e^{i\mathbf{k}\mathbf{r}} e^{-(\mathbf{v}\cdot\mathbf{k})^2/4}}{\sum_{\mathbf{k}} C_n(\mathbf{k}) (n - 2m') e^{i\mathbf{k}\mathbf{r}} e^{-(\mathbf{v}\cdot\mathbf{k})^2/4}} \quad (45)$$

The derivatives leave the exponentials intact but bring down factors of $n - 2m$ in the numerator and $n - 2m'$ in the denominator. The exponential terms are the key to the unusual behavior seen in Figure 10. With x and y chosen generically, and r large with $\alpha = r \cos \theta$, $\beta = r \sin \theta$, typically one of the exponential terms will dominate the others, infinitely so as $r \rightarrow \infty$. Because the real exponents $-(\mathbf{v}\cdot\mathbf{k})^2$ are negative definite, the dominating exponential will have the smallest magnitude of the projection $\mathbf{v}\cdot\mathbf{k}$.

The integer n must be even so that the potential is a periodic lattice of positive bumps. Let $j = n/2$. Then the ordered sequence of different irreducible rationals $0 \leq p/q \leq 1$ for $q \leq k$ obtainable from the list $|(n - 2m)/(n - 2m')|$, $0 \leq m' \leq m \leq n$ is the *Farey sequence* of rationals, F_j .²⁰ The Farey sequence for any positive integer n is the set of irreducible rational numbers p/q with $0 \leq p \leq q \leq n$ and arranged in increasing

order. The Farey sequence is intimately related to rational approximants to irrational numbers. The closest continued fraction approximants to a given irrational number γ of order j (i.e., largest denominator j) are the Farey rationals closest to γ .

The Farey rationals $F_{n/2}$ (and their inverses) determine the resonance for a given n . That is, when the rational plateau is

$$\frac{p}{q} = \frac{n - 2m}{n - 2m'} \quad (46)$$

then on resonance the condition

$$\frac{\alpha}{\beta} = -\frac{q}{p} \quad (47)$$

holds. This resonance point is not usually at the center of the plateau. The edges of the resonance plateau, i.e., the transition point between different resonances, can be found as follows. Let $p_1/q_1, p_2/q_2$ be two neighboring rational fractions in a Farey sequence of order $j = n/2$. On resonance 1, we have $\alpha q_1 + \beta p_1 = 0$, and on resonance 2, $\alpha q_2 + \beta p_2 = 0$. At the transition point between the two resonances, neither projection will vanish but instead they will be of equal magnitude but opposite in sign, i.e., $\alpha q_1 + \beta p_1 = -(\alpha q_2 + \beta p_2)$. This means that the transition point marking the jump between plateaus of resonance 1 and resonance 2 is at

$$\frac{\alpha}{\beta} = -\frac{(p_1 + p_2)}{(q_1 + q_2)} \quad (48)$$

which it turns out is the definition of the *mediant* of the two adjacent rational fractions. The mediant is the first intermediate rational fraction that appears between the two in question in a higher Farey sequence, F_j . (For the purpose of the mediant, the first rational in each Farey sequence, namely 0, is considered to be 0/1, and the last is 1/1.) We have thus found that a given resonance plateau p/q will hold from the lower mediant to the upper mediant bracketing the corresponding rational fraction.

We recall that for the transitions from one plateau to another to be sharp, we must take the limit of an adiabatic perturbation, i.e., $\alpha^2 + \beta^2 \rightarrow \infty$. In this limit the perturbation turns on and off slowly compared to the time required to pass from one unit cell to another. Figure 10 shows the ratio $\Delta p_x/\Delta p_y$ as a function of the incident angle θ for $\eta = 20$ and for two different velocities, $|\mathbf{v}| = 10$ and $|\mathbf{v}| = 125$, calculated from eq 45. The lower velocity case accesses only a few unit cells of the lattice during the time the perturbation is on, whereas the higher one is more nearly adiabatic, displaying all the plateaus predicted for $\Delta p_x/\Delta p_y$ for the Farey sequence F_{10} . The jumps between plateaus are indeed at the mediant angles. For the short duration case, there are sloppy transitions between the plateaus, many of which are missing or indistinct. Only the lowest order resonances survive as well formed plateaus. This can be understood as follows. Consider the two unperturbed trajectories shown in Figure 11, where a rectangular lattice of soft points is shown together with two weighted trajectory tracks, one at $\tan \theta = 1$ and the other at $\tan \theta = 1/4$. In both cases the impulse is perpendicular to the track, but the 1:1 track is much more adiabatic, suffering more collisionettes (interactions with individual lattice points) during the time the interaction is on (the interaction strength is indicated by the shading on the track). For a given duration time of the interaction, sufficiently high order resonances will not be able to establish themselves through multiple collisionettes. The condition for a plateau p/q to appear

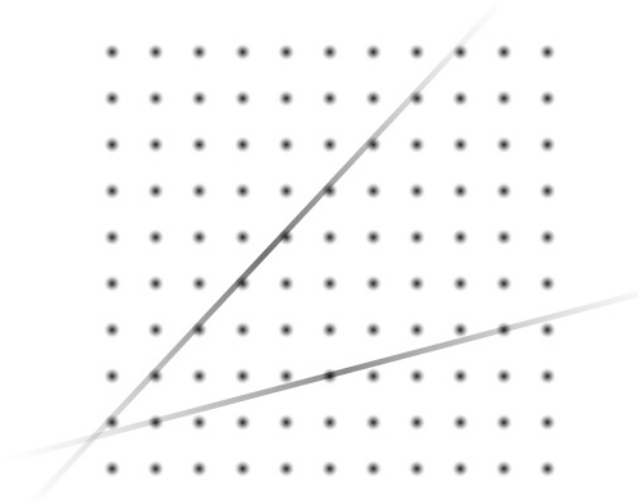


Figure 11. Rectangular lattice of soft points shown together with two weighted tracks, one at one at $\tan \theta = 1$ and the other at $\tan \theta = 1/4$. In both cases the impulse will be perpendicular to the track, but the $\tan \theta = 1$ track is much more adiabatic, suffering more collisionettes (interactions with individual lattice points) during the time the interaction is on (the interaction strength is indicated by the shading on the track).

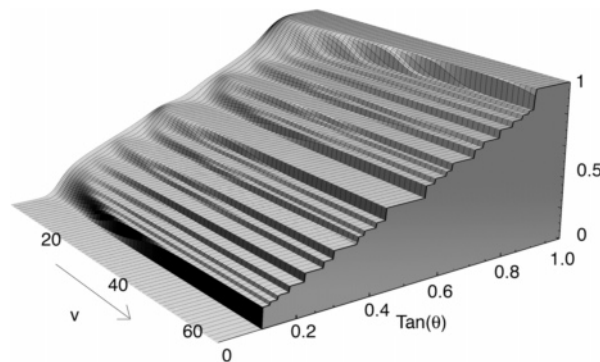


Figure 12. Formation of the Devil's Staircase for $\eta = 16$, as a function of the velocity $v = |\mathbf{v}|$, assuming the interaction time goes as $\exp[-t^2]$.

(assuming again a time profile $\sim \exp[-t^2]$) is

$$|\mathbf{v}| \gg \sqrt{p^2 + q^2}$$

Comparison with the explicit nonperturbative calculations of the previous section is instructive. Figure 6 and Figure 8 refer to the case $\eta = 2$. The perturbative result for $\eta = 2$ shows peaks only at $F_1 = \tan \theta = \{0, 1\}$. The additional peaks and plateaus seen at $1/3, 1/2$, etc. are the result of higher order processes included in the full numerical integration of the trajectories. Similar statements may be made about the extra peaks seen in the case $\eta = 6$.

Suppose $\omega_{\text{def}} = \omega_2 - M/N\omega_1$ differs somewhat from 0, and that a higher order resonance $\omega'_{\text{def}} = \omega_2 - M'/N'\omega_1$ is closer to 0. Which resonance will hold? Within perturbation theory, the Fourier components of the perturbation have to generate the fraction M'/N' as part of the Farey sequence if it is to compete with M/N . (Higher order interactions can do that from a lower order potential, as was seen in the explicit numerical investigation of section 4.) Assuming that is the case, the M/N plateau will actually never appear in the situation above: quasiresonance will fail until the interaction time is long enough to resolve the M'/N' plateau. Figure 12 reveals that, as the adiabaticity is increased (i.e., the velocity v of the particle is increased) new

plateaus form from smooth, unquantized regions in the ratio of actions, not from other, lower order plateaus which formed earlier. This mechanism could change for other forms of the perturbation.

It can easily happen that *both* actions are adiabatic, e.g., when no low order resonance condition applies. Then there are two nearly good constants of the motion, but the ratio of the very small action changes will not plateau, because there is no resonance condition to enforce the action ratio.

7. Quasiresonance in Higher Dimensional Systems

From a broader perspective, quasiresonance is a side effect of the adiabaticity of classical actions that may arise under slow perturbations. Already in one dimension, adiabaticity of the action may or may not be guaranteed for slow variation of a parameter, depending on whether a separatrix and its attendant zero classical frequencies are present. For a two-dimensional classical system, subject to a time dependent perturbation, the resonance condition $N\omega_2 - M\omega_1 \approx 0$ implies a slow angle whose conjugate action will not be conserved, and a fast angle with possible conservation of an action of the form $I_2 = J_2 + (M/N)J_1$. The slow degree of freedom develops separatrices and violates adiabaticity. This gives the quasiresonance condition relating ΔJ_1 and ΔJ_2 : $\Delta J_1/\Delta J_2 = -N/M$. Thus, in more than one dimension, something of interest survives even if some of the actions are not adiabatic. In higher dimensions, one quantity of interest will hold for each conserved action, i.e., for each "fast" angle. Mixing could in principle be quite strong among the slow angles over the course of the perturbation.

The quantities of interest in higher dimensions are more conveniently the conserved rational combination of actions. These could be discovered from data. Indeed, this was the case for the original vib-rotor quasiresonance.¹ It is possible that higher order quasiresonance lies hidden in existing data sets, because a rational condition involving three or four action changes might easily go unnoticed.

Quasiresonance may be a useful way to explore Arnold diffusion,²¹ which is a presumably slow process of action diffusion in quasi-integrable systems of three and more degrees of freedom. Unlike two-dimensional systems where KAM surfaces divide phase space, three and higher dimensional systems can bypass such surfaces by going around them, because they are of co-dimension two and higher, and can be avoided the same way a line can be avoided in three dimensions. The mechanism for this is the Arnold web, in which surface manifolds obeying a resonance condition intersect along lower dimensional manifolds where two or more resonances prevail. A phase space point can take a turn there, deciding to follow a new resonance.

8. Conclusion

In a previous paper,¹² we quantified the theory of quasiresonance, gave further examples, and showed that the effect holds both for the original autonomous systems and for nonautonomous ones as well. The present paper has further expanded the theory, uncovering the number theoretical foundations of

quasiresonance in the perturbative limit and stronger collisions, and investigating a realistic potential for He-H₂ collisions.

We have suggested some directions for future work on higher dimensional systems, including Arnold diffusion. This remains a largely unexplored territory, however.

Another possibility deserving more attention is the transient interaction with a perturbation and a system that possesses a complex phase space replete with resonance zones, etc., even in the absence of the perturber. Under very weak interactions, this case does fall under the integrable limit with good actions, because that is effectively the situation in very local regions of phase space. We have not treated the case where the definition of the *unperturbed* actions changes over some region of phase space and mixing occurs over a region at least as large.

Acknowledgment. E.J.H. thanks a friend and colleague, Jack Simons, for crucial encouragement and resonant inspiration over the course of many years. His wide ranging talents, interests, and efforts on behalf of theoretical chemistry are deeply appreciated. A.R. thanks Robert Parrott, Diego V. Bevilaqua, and Daniel Alonso for many fruitful discussions. A.R. gratefully acknowledges the hospitality of the Physics Department of Harvard University, where the present work was carried out. We thank the referee for helpful comments and suggestions. A.R. was supported by a Fulbright/MECD grant from Secretaría de Estado de Educación y Universidades and, partially, from Fondo Social Europeo. This work was also supported by a grant from the National Science Foundation, NSF CHE-0073544.

References and Notes

- (1) Stewart, B.; Magill, P. D.; Scott, T. P.; Derouard, J.; Pritchard, D. E. *Phys. Rev. Lett.* **1988**, *60*, 282.
- (2) Magill, P. D.; Stewart, B.; Smith, N.; Pritchard, D. E. *Phys. Rev. Lett.* **1988**, *60*, 1943.
- (3) Magill, P. D.; Scott, T. P.; Smith, N.; Pritchard, D. E. *J. Chem. Phys.* **1989**, *90*, 7195.
- (4) Scott, T. P.; Smith, N.; Magill, P. D.; Pritchard, D. E. *J. Phys. Chem.* **1996**, *100*, 7981.
- (5) Levine, R. D.; Bernstein, R. B. *Molecular Reaction Dynamics and Chemical Reactivity*, 2nd ed.; Oxford University Press: Oxford, U.K., 1987; p 334.
- (6) Hoving, W. J.; Parson, R. *Chem. Phys. Lett.* **1989**, *158*, 222.
- (7) Forrey, R. C.; Balakrishnan, N.; Dalgarno, A.; Haggerty, M. R.; Heller, E. J. *Phys. Rev. Lett.* **1999**, *82*, 2657.
- (8) Clare, S.; McCaffery, A. J. *J. Phys. B* **2000**, *33*, 1121.
- (9) Forrey, R. C. *Phys. Rev. A* **2001**, *63*, 051403.
- (10) Forrey, R. C. *Phys. Rev. A* **2002**, *66*, 023411.
- (11) Flasher, J. C.; Forrey, R. C. *Phys. Rev. A* **2002**, *65*, 032710.
- (12) Ruiz, Antonia; Heller, E. J. *J. Mol. Phys.*, in press.
- (13) Lichtenberg, A. J.; Leiberman, M. A. *Regular and Chaotic Dynamics*; Springer-Verlag: New York, 1992.
- (14) Skodje, R. T.; Borondo, F.; Reinhardt, W. P. *J. Chem. Phys.* **1985**, *82*, 4611.
- (15) Forrey, R. C.; Balakrishnan, N.; Dalgarno, A.; Haggerty, M. R.; Heller, E. J. *Phys. Rev. A* **2001**, *66*, 022706.
- (16) Schwenke, D. W. *J. Chem. Phys.* **1988**, *89*, 2076.
- (17) Muchnick, P.; Russek, A. *J. Chem. Phys.* **1994**, *100*, 4336.
- (18) Miklavc, A. *J. Chem. Phys.* **2001**, *114*, 10980.
- (19) McCaffery, M. J. *J. Chem. Phys.* **1999**, *111*, 7697.
- (20) Weisstein, Eric W. Farey Sequence. From MathWorld-A Wolfram Web Resource. <http://mathworld.wolfram.com/FareySequence.html>.
- (21) Lichtenberg, A. J.; Lieberman, M. A. *Regular and Chaotic Dynamics*; Springer-Verlag: New York, 1992.